Available online at www.sciencedirect.com
SCIENCE DIRECT®
Physica C 406 (2004) 100–106
PHYSICA C
www.elsevier.com/locate/physc

Effect of hydrogen uptake and substrate orientation on the flux penetration in NbH_x thin films

M.S. Welling *, C.M. Aegerter, R.J. Westerwaal, S. Enache, R.J. Wijngaarden, R. Griessen

Division of Physics and Astronomy, Faculty of Sciences, Vrije Universiteit, De Boelelaan 1081, 1081 HV Amsterdam, The Netherlands

Received 15 December 2003; received in revised form 17 March 2004; accepted 18 March 2004
Available online 16 April 2004

Abstract

By absorbing various amounts of hydrogen in the same niobium sample we are able to change the local superconducting properties thus introducing quenched disorder in a controlled manner. Its effect on the magnetic flux penetration in NbH_x thin films on *A*-plane $(1\,1\,\bar{2}\,0)$ and *R*-plane $(1\,\bar{1}\,0\,2)$ sapphire substrates is systematically investigated using a magneto-optical technique. With increasing hydrogen content, flux penetration patterns are observed to become more irregular. At high hydrogen concentrations non-superconducting inclusions are formed. The substrate orientation also has a strong influence on the observed behavior, revealing line-shaped avalanches at 4.2 K for *A*-plane substrates and a more continuous but spatially irregular behavior for *R*-plane substrates.

PACS: 45.70.Qj; 45.70.Ht; 74.78.Db; 74.25.Qt; 68.55.Ln
Keywords: Magneto-optical; Niobium; Hydrogen impurities; Thermo-magnetic avalanches

1. Introduction

Recently it has become clear that the flux penetration in type-II superconductors may deviate in detail from the Bean critical state [1]. This may lead to roughening of the flux front [2] or even to pronounced dendritic flux penetration patterns [3]. Surprisingly, for niobium different authors have reported quite different flux penetration behavior. In classic magneto-optical (MO) studies by Huebener et al. [4] rather smooth and regular Bean-like flux penetration is observed in thin foils, while they found filamentary, seaweed-like patterns in sputtered thin films [4]. Finger-like patterns are reported by Aoki and Habermeier [5] and Rowe et al. [6] whereas dendritic patterns are observed by Duran et al. [7], who used sputtered niobium films on various kinds of substrates. Finally, rather irregular, 'rough' Bean-like flux patterns are reported by James et al. [8] on sputtered samples. We suspect that these differences arise due to the different defect structure of the investigated samples. To verify this assumption experimentally, we exploit the fact that niobium easily absorbs hydrogen, which locally destroys the superconductivity,

* Corresponding author. Tel.: +31-20-4447923; fax: +31-20-4447992.
E-mail address: welling@nat.vu.nl (M.S. Welling).

0921-4534/$ - see front matter © 2004 Elsevier B.V. All rights reserved.
doi:10.1016/j.physc.2004.03.236

by changing the amount of (interstitially) absorbed hydrogen in the same sample thus introducing static pinning sites. Thus we can vary the amount of defects in a controlled manner. In our experiment we study the flux penetration patterns in niobium by magneto-optics [9] for different hydrogen concentrations. Since sapphire is widely used as substrate, we focus our efforts on niobium films grown on *A*- and *R*-plane sapphire substrates.

The paper is organized as follows. In the next section the sample, the hydrogenation and the magnetic field sweep procedure as well as the MO set-up are presented. In Section 3, we show the influence of the substrate orientation on the magnetic field distribution. In Section 4, we show the change of behavior induced by increasing hydrogen doping. In Section 5, we discuss morphological changes of the surface due to the increasing hydrogen content. We end with a summary of the main results and a discussion.

2. Experimental

Niobium thin films of 500 nm thickness are epitaxially grown on *A*-plane $(1\,1\,\bar{2}\,0)$ and *R*-plane $(1\,\bar{1}\,0\,2)$ sapphire substrates. The substrates are cleaned with demi-water, acetone, and an ultrasonic ethanol bath. Subsequently, they are baked out at 973 K. Evaporation of the niobium with a growth rate of 0.5 Å/s is done at 973 K under ultrahigh vacuum (UHV) conditions (base pressure 2×10^{-7} Pa) using molecular-beam epitaxy (MBE). The well known epitaxial relationship between niobium and sapphire [10] is confirmed by X-ray measurements on the as-grown films on *A*- and *R*-plane substrates. For *A*-plane sapphire we find that the $(1\,1\,0)$ plane of Nb grows epitaxially on the $(1\,1\,\bar{2}\,0)$ plane of the sapphire substrate with $[1\,\bar{1}\,1]_{\mathrm{Nb}}\|[0\,0\,0\,1]_{\mathrm{Al_2O_3}}$. For *R*-plane sapphire we find that the $(0\,0\,1)$ plane of Nb grows epitaxially on the $(1\,\bar{1}\,0\,2)$ plane of the sapphire substrate with $[1\,1\,0]_{\mathrm{Nb}}\|[1\,1\,\bar{2}\,0]_{\mathrm{Al_2O_3}}$. We use a shadow mask to obtain a strip geometry of 9.0×1.8 mm^2, avoiding possible contamination of niobium by hydrogen during post-deposition wet-etching patterning. Niobium forms an oxide layer when exposed to air, which is hardly permeable to hydrogen. To be able to introduce hydrogen into the films in a controlled manner, we evaporate a 10 nm thick Pd cap layer on top of the niobium film at room temperature but still under UHV conditions. Palladium protects the film from oxidation and catalytically dissociates the H_2 molecules into H atoms that diffuse easily into the niobium film. From the measured hydrogen partial pressure in the UHV system we estimate the hydrogen concentration in the as-grown films to be less than 0.1%. Before increasing the hydrogen concentration, we determined the critical temperature $T_c = 9.22(5)$ and the tangent $-\mu_0\,\mathrm{d}H_{c_2}(T)/\mathrm{d}T = 0.123(1)$ T/K at $T = T_c$ to obtain an estimate [11] for the upper critical field at zero temperature of $\mu_0 H_{c_2} = 0.6$ T for the sample on the *A*-plane substrate. For the sample on the *R*-plane substrate we determined $T_c = 9.00(5)$ and $-\mu_0\,\mathrm{d}H_{c_2}(T)/\mathrm{d}T = 0.074(1)$ T/K at $T = T_c$ leading to an estimate [11] for the upper critical field at zero temperature of $\mu_0 H_{c_2} = 0.3$ T.

In the experiments presented here, the local magnetic flux density (B_z) immediately above the superconducting sample is measured using our magneto-optical image lock-in amplifier (MOILIA [9]). This is achieved by detecting the polarization change in a Bi-substituted ferrite–garnet film [12] with in-plane magnetization vector and large Faraday effect (typically 0.06 deg/mT). This 'indicator' is mounted on top of the sample. The assembly consisting of sample and indicator is mounted in a specially built cryogenic polarization microscope, which fits into the variable temperature insert of an Oxford Instruments 1-T magnet system. In addition to the hydrogen gas inserted into the sample space, a small amount of helium gas (partial pressure 6×10^3 Pa) is used as a contact gas. Before cooling down, we wait 1 h (at room temperature) to equilibrate the hydrogen concentration throughout the sample. The externally applied magnetic field is perpendicular to the sample and indicator surface. Experiments are performed at 4.2 and 6.7 K after zero field cooling (ZFC). The externally applied magnetic field is increased from 0 to 20 mT in steps of 50 μT, using a constant sweep rate of 50 μT/s between steps. After every field step, the flux distribution in the

sample is relaxed for 3 s after which a MO image is acquired. We investigate only the middle part of the sample, to avoid geometrical effects due to the corners. The pictures are taken with a charge-coupled device camera (with 782×582 pixels) using an exposure time of 300 ms. The spatial resolution is such that one side of a square pixel corresponds to 3.4 μm. After the final acquired MO image, the field is removed and the sample is heated up above T_c and cooled down again, after which the experiment is repeated to investigate the reproducibility. Next, the sample is heated up to room temperature. Subsequently the sample space is flushed and the hydrogen content in the sample increased further by applying about twice the previously applied hydrogen pressure.

3. Effect of substrate orientation

We now discuss the qualitatively different magnetic field patterns in niobium thin films on *A*-plane and *R*-plane sapphire substrates. The magnetic flux distribution in a niobium thin film on an *A-plane substrate* after ZFC to 4.2 K at an applied field of 6.8 mT is shown in Fig. 1(a). The Meissner phase appears black and the Shubnikov phase bright. With increasing magnetic field, the flux enters in instantaneous bursts (on our experimental time scale), forming finger-like protrusions with initially little branching. At higher magnetic field we observe an increase in branching. With increasing density of the flux fingers, we observe an apparent repulsive interaction between neighboring fingers, which leads to the development of a more complex flux distribution pattern, where more meandering, branching, and twisting of magnetic flux fingers is observed. Above a certain threshold temperature (≈6.2 K), flux penetrates in a smoother manner. This behavior is consistent with the occurrence of thermo-magnetic avalanches proposed by Aranson et al. [13], where branching of the penetrating flux occurs when it encounters a defect. A more detailed experimental investigation of the behavior in the *A*-plane case will be presented elsewhere [14].

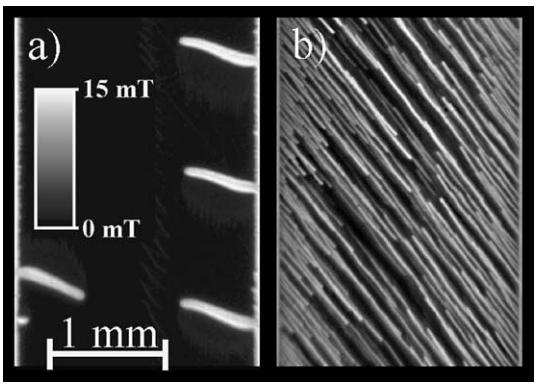

Fig. 1. Magnetic flux distribution in a 500 nm Nb thin film on an *A*-plane substrate after zero field cooling to 4.2 K and subsequently applying a field of 6.8 mT. (a) The as-grown film, (b) the same film after exposure to hydrogen gas at a pressure of 60 Pa. The black area corresponds to the Meissner phase, and bright regions to the Shubnikov phase. The magnetic flux distribution in (a) shows finger-like flux protrusions, which enter the sample in an abrupt manner and (b) shows easy flow channels (see text).

In Fig. 2(a), the magnetic flux distribution in a niobium thin film on a *R-plane substrate* after ZFC to 4.2 K at an applied field of 6 mT is shown. With increasing magnetic field, flux enters in a gradual manner, and large avalanches are absent. The slow driving of the magnetic flux, due to the slow ramping up of the magnetic field causes flux to penetrate in the form of small plumes, which form a 'rough' flux front (borderline between Meissner and Shubnikov phase). Below we investigate the influence of hydrogen impurities.

4. Effect of hydrogen impurities

To investigate the effect of impurities on the flux penetration patterns we use the fact that niobium easily absorbs hydrogen. This property is well known, however the effects of hydrogen on the superconducting properties [15] of niobium films have not been investigated in great detail. It is well known that hydrogen doping causes significant modifications of the electronic, magnetic, and structural properties due to the interaction of hydrogen with the host film. The lattice expansion due to hydrogen uptake [16] induces structural changes such as crystal lattice distortions, dislocations [17] and morphological changes. We now discuss the various different phases that can be

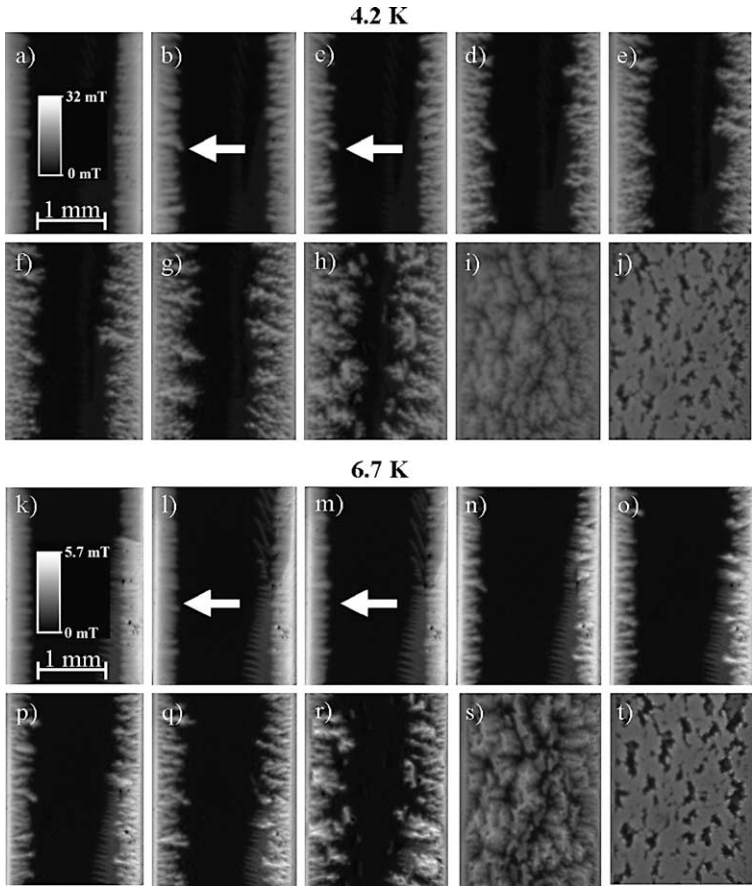

Fig. 2. (a)–(j) Magnetic flux distribution in a 500 nm thick Nb thin film on an *R*-plane substrate after zero field cooling to 4.2 K and subsequently applying a field of 6 mT; (k)–(t) the behavior after zero field cooling to 6.7 K and subsequently applying a field of 1.5 mT. (a,k) The as-grown film, (b)–(j) and (l)–(t) show the same region after exposure to hydrogen gas pressures of 80, 260, 1130, 1280, 1810, 3440, 6750, 12,800, and 40,000 Pa. Note that the hydrogen content of the sample is increased by applying hydrogen gas pressure at room temperature. After zero field cooling, the complete evolution of the magnetic flux penetration with increasing magnetic field is obtained. The black area corresponds to the Meissner phase, and bright regions to the Shubnikov phase. The arrows in (b) and (c) indicate the growth of a branching magnetic flux protrusion with increasing hydrogen content at 4.2 K, which is absent in (l) and (m) at 6.7 K (see text). The zigzag pattern, visible in the 6.7 K images, is an artifact of the MO-indicator.

expected to be formed based on the bulk phase diagram [18]. For low hydrogen concentrations and temperature around room temperature (where we change the hydrogen concentration), the α phase is formed, which is a disordered solution of hydrogen in bcc niobium. At somewhat higher hydrogen concentrations, the $\alpha + \beta$ phases coexist. The β phase is an ordered interstitial solid solution of hydrogen. It is important to note that the β phase is not superconducting above 1.2 K [18,19], while the lowest temperature investigated here is 4.2 K. Upon cooling down to 4.2 K the ϵ phase forms. Randomly distributed precipitates of ϵ phase with typical sub-micrometer size are formed. Thus at low temperature we expect the $\alpha + \epsilon$ phases with possibly (at high hydrogen concentrations) β phase regions. We present now the results for the niobium films on *A*-plane substrates. The results of the films on *R*-plane substrates are given at the end of this section.

In Fig. 1(b), we show the magnetic flux distribution in a niobium film on an *A-plane substrate*

after loading with hydrogen at a hydrogen gas pressure of 60 Pa at room temperature. The sample is ZFC to 4.2 K and subsequently a magnetic field of 6.8 mT is applied. Black areas correspond to the Meissner phase and bright regions to the Shubnikov phase. The magnetic flux penetrates still in a burst-like manner through channels, but these are much narrower and more closely spaced than in a sample without hydrogen. Note also the change of direction of entering flux with increased hydrogen content.

Fig. 2(a)–(j) show the magnetic flux distribution in a niobium thin film on a *R-plane substrate* after ZFC to 4.2 K and subsequently applying a magnetic field of 6 mT. The hydrogen content of the sample is increased in Fig. 2(b)–(j) by applying a hydrogen gas pressure of 80, 260, 1130, 1280, 1810, 3440, 6750, 12,800, and 40,000 Pa at room temperature. Thus with every experiment the sample is increasingly loaded with hydrogen. Subsequently (after ZFC), the complete evolution of the magnetic flux penetration, due to increasing the externally applied magnetic field, is recorded. The magnetic field entering the as-grown film is shown in Fig. 2(a), together with a gray-scale bar indicating the local magnetic flux density B_z that holds for Fig. 2(a)–(j). The flux penetrates in the form of (white) small plumes, which form a 'rough' flux front. With growing hydrogen content, the flux penetration becomes more irregular and changes radically, see Fig. 2(b)–(g). For example, the arrows in Fig. 2(b) and (c) point at one magnetic flux protrusion which splits more and more with increasing hydrogen concentration. Note that flux penetrates further into the superconductor with increasing hydrogen content. This corresponds to an overall decrease of the critical current. The complete loss of superconducting properties over macroscopic regions is clearly visible in Fig. 2(h). This change is probably due to the formation of β-phase, thus creating macroscopic non-superconducting inclusions, which grow with increasing hydrogen content. In Fig. 2(j), we observe flux penetration in disconnected superconducting regions, which appear as black regions with bright surrounding: the connection between neighboring superconducting regions is completely lost. The observed bright area in between the black areas indicates that the local magnetic field in these regions is equal to the externally applied magnetic field (and hence that these regions are non-superconducting). Fig. 2(k)–(s) show experiments performed at 6.7 K at the same hydrogen gas pressures as above, where we applied a (lower) magnetic field of 1.5 mT in order to be able to compare the evolved flux front with the 4.2 K case due to the decrease in critical current with temperature. In Fig. 2(k) we added a scale bar indicating the local magnetic flux density B_z that holds for Fig. 2(k)–(s). Again, a bumpy flux front is present in the as-grown film shown in Fig. 2(k). It is remarkable that the flux front remains much smoother for increasing hydrogen content. The arrows in Fig. 2(l) and (m) indicate the same position as in Fig. 2(b) and (c), but now the growth of a branching magnetic flux protrusion with increasing hydrogen content is completely absent. Apparently, the onset of the increase in irregularity of the penetrating flux front for increasing hydrogen concentration is shifted to higher hydrogen concentration with increased temperature.

5. Surface morphology

We now discuss the influence of hydrogen uptake on the surface morphology for both substrate orientations. In the *A*-plane case hydrogen uptake at 60 Pa gas pressure results in the formation of a wavy pattern at the surface. Our polarized light photographs of this morphology are made at room temperature, and are shown in Fig. 3(a). The MO experiment in Fig. 3(b) (see also Fig. 1(b)), clearly shows that the magnetic flux follows easy flow channels that are parallel to the structural pattern of Fig. 3(a). This shows that vortex pinning is governed by the waviness of the observed surface pattern, resulting in flux guidance through channels with identical orientation as the morphological wave pattern. In Fig. 3(d), we show a polarized light photograph of the *R*-plane sample at room temperature after exposure to 40,000 Pa hydrogen gas pressure together with a MO picture (Fig. 3(e)) of the same area. A careful comparison of the surface morphology Fig. 3(d) with the MO image Fig. 3(e) leads to the conclusion that there is

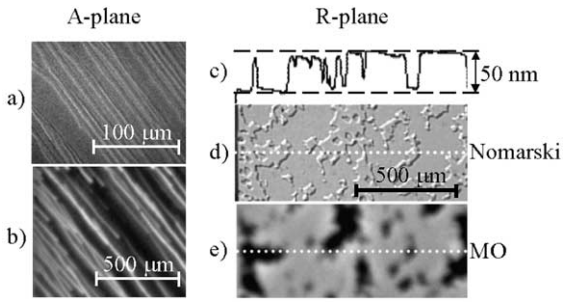

Fig. 3. Comparison between superconducting properties and surface morphology. The surface morphology in (a) and (d) is measured at room temperature using polarized light microscopy while (b) and (e) are MO images. (a) Surface morphology of a 500 nm thick Nb film on an *A*-plane substrate after exposure to 60 Pa hydrogen gas pressure revealing the presence of a wavy surface pattern. (b) Corresponding magnetic flux distribution observed by MO. (c) Height profile scan of the Nb film on an *R*-plane substrate, revealing islands with a 10% (50 nm) out-of-plane expansion due to the formation of the β-phase at a hydrogen gas pressure of 40,000 Pa. The profile was measured along the dotted white line indicated in (d) and (e). (d) Surface morphology of *R*-plane sample in the same area as the MO picture shown in (e). Note the nice correlation between the loss of superconductivity (in the bright area in figure (e)), and the height increase in (d).

a one-to-one correlation between the out-of-plane expansion and the local disappearance of superconducting properties (as expected for the formation of the β phase).

To obtain absolute height information of the sample surface, height profile scans along the dotted white line in Fig. 3(d) and (e) were made before and after hydrogenation using a DEKTAK height profile scanner. The hydrogen uptake results in an out-of-plane expansion of 10% (corresponding to 50 nm) as shown in Fig. 3(c). From several height profiles we find that on average 67(6)% of the investigated area expanded in the out-of-plane direction. This implies [16] an overall hydrogen concentration (atomic ratio H/Nb) between around 0.5 and 1.0 for the 40,000 Pa exposure showing that we have covered a large range of hydrogen concentrations in NbH_x by the present experiments.

6. Summary

We investigate flux penetration in NbH_x thin films on sapphire substrates with different orientation and for various hydrogen content and find large qualitative changes in the magnetic flux penetration pattern. We demonstrate that for our as-prepared "hydrogen-free" samples the substrate orientation has a strong influence on the flux penetration behavior, revealing finger-like avalanches for the *A*-plane orientation and a more continuous flux penetration for the *R*-plane. We find hardly any branching of the avalanches in the *A*-plane case at 4.2 K. Hydrogen absorption at room temperature modifies the observed behavior significantly for hydrogen pressures above $\simeq$60 Pa. In the *A*-plane case at low concentrations, hydrogen induces surface morphological changes inducing flux flow along easy flow channels. In the *R*-plane case at low concentrations, hydrogen leads to irregular flux penetration. At high concentrations non-superconducting inclusions are created due to the formation of the β phase, finally leading to the fragmentation of the superconductor into separated superconducting islands. We find a one-to-one correlation between the superconducting properties and the local out-of-plane expansion. Furthermore, comparing the 4.2 K with the 6.7 K experimental series, we conclude that with increasing temperature the evolving flux pattern is smoother. The fact that we observe the significant change in behavior only at hydrogen pressures above 60 Pa implies that the already present quenched disorder in the as-grown films dominates for lower hydrogen gas pressures. Thus differences in behavior reported in the literature must be mainly due to differences in quenched disorder caused by some other cause such as growth conditions, substrate quality, and substrate orientation etc.

Finally, NbH_x thin films on *R*-plane substrates offer interesting possibilities for the study of roughening phenomena such as are e.g. observed in the study of the movement of an interface in a disordered medium (such as the edge of ink in blotting paper). There the velocity of the interface is affected by spatially distributed but time independent inhomogeneities in the medium. The possibility to change this quenched disorder in the same medium (by changing the hydrogen content) and study the robustness of the roughening behavior is of great interest. Thus the possibility to

add a well-controlled amount of disorder in niobium thin films on *R*-plane substrates makes NbH_x an ideal system to study the influence of quenched disorder on roughening phenomena [2,20].

Acknowledgements

We would like to thank Nico Koeman for the samples and Arndt Remhof for useful discussions. This work was supported by FOM (Stichting voor Fundamenteel Onderzoek der Materie), which is financially supported by Nederlandse Organisatie voor Wetenschappelijk Onderzoek (NWO). We acknowledge the European Science Foundation (ESF) VORTEX Program for support.

References

[1] C.P. Bean, Rev. Mod. Phys. 36 (1964) 31.
[2] R. Surdeanu, R.J. Wijngaarden, E. Visser, J.M. Huijbregtse, J.H. Rector, B. Dam, R. Griessen, Phys. Rev. Lett. 83 (1999) 2054.
[3] R.V. Bujok, P. Brüll, J. Boneberg, S. Herminghaus, P. Leiderer, Appl. Phys. Lett. 63 (1993) 412.
[4] R.P. Huebener, V.A. Rowe, R.T. Kampwirth, J. Appl. Phys. 41 (1970) 2963.
[5] R. Aoki, H.U. Habermeier, Jpn. J. Appl. Phys. 26 (1987) 1453.
[6] V.A. Rowe, R.P. Huebener, R.T. Kampwirth, Phys. Stat. Sol. (a) 4 (1971) 513.
[7] C.A. Duran, P.L. Gammel, R.E. Miller, D.J. Bishop, Phys. Rev. B 52 (1995) 75.
[8] S.S. James, S.B. Field, J. Seigel, H. Shtrikman, Physica C 332 (2000) 445.
[9] R.J. Wijngaarden, K. Heeck, M. Welling, R. Limburg, M. Pannetier, K. van Zetten, V.L.G. Roorda, A.R. Voorwinden, Rev. Sci. Instrum. 72 (2001) 2661.
[10] K. Yoshii, H. Yamamoto, K. Saiki, A. Koma, Phys. Rev. B 52 (1995) 13570.
[11] N.R. Werthamer, E. Helfand, P.C. Hohenberg, Phys. Rev. 147 (1966) 295.
[12] L.A. Dorosinskii, M.V. Indenbom, V.I. Nikitenko, Y.A. Ossipyan, A.A. Polyanskii, V.K. Vlasko-Vlasov, Physica C 203 (1992) 149.
[13] I. Aranson, A. Gurevich, V. Vinokur, Phys. Rev. Lett. 87 (2001) 067003.
[14] M.S. Welling, R.J. Wijngaarden, in preparation.
[15] L.Ya. Vinnikov, O.V. Zharikov, Ch.V. Kopetskii, V.M. Polovov, Sov. J. Low Temp. Phys. 3 (1977) 4.
[16] G. Song, A. Remhof, D. Labergerie, H. Zabel, Phys. Rev. B 66 (2002) 045407;
G. Song, A. Remhof, K. Theis-Bröhl, H. Zabel, Phys. Rev. Lett. 79 (1997) 5062;
G. Song, M. Geitz, A. Abromeit, H. Zabel, Phys. Rev. B 54 (1996) 14093.
[17] C.P. Herring, J. Phys. F: Metal Phys. 6 (1976) 99.
[18] G. Alefeld, J. Völkl, Hydrogen in Metals II, Topics in Applied Physics, vol. 29, Springer-Verlag, 1978.
[19] J.M. Welter, F.J. Johnen, Z. Physik B 27 (1997) 227.
[20] M.S. Welling, C.M. Aegerter, R.J. Wijngaarden, Phys. Rev. Lett., to appear.